Block Copolymers

International Edition: DOI: 10.1002/anie.201504136
German Edition: DOI: 10.1002/ange.201504136

Self-Healing Materials from V- and H-Shaped Supramolecular Architectures**

*Senbin Chen, Nasir Mahmood, Mario Beiner, and Wolfgang H. Binder**

Dedicated to Professor Rolf Mülhaupt on the occasion of his 60th birthday

Abstract: *Integrating self-healing capability into supramolecular architectures is an interesting strategy, and can considerably enhance the performance and broaden the scope of applications for this important class of polymers. Herein we report the rational design of novel V-shaped barbiturate (Ba) functionalized soft–hard–soft triblock copolymers with a reversible supramolecular healing motif (Ba) in the central part of the hard block, which undergoes autonomic repair at 30°C. The designed synthesis also offers a suitable macromolecular building block to further self-assemble with heterocomplementary α,ω-Hamilton wedge (HW) functionalized polyisoprene (PI; HW-PI-HW), resulting in an H-shaped supramolecular architecture with efficient self-healing capabilities that can recover up to around 95% of the original mechanical performance at 30°C within 24 h.*

The design of polymers with multiple self-healing properties[1] is an important topic and has generated a number of different concepts, many of them related to the exploitation of transient (supramolecular) bonds displaying dynamic properties.[2] If such bonds are incorporated in the materials through networks or clusters, their inherent dynamic nature allows the repair of damage, even at the same position, leading to multiple self-healing. Hydrogen-bonding systems,[3] metal complexes,[4] as well as reversible bonds with a low activation energy[5] (e.g., disulfides or nitroxides, which possess dynamic properties even at room temperature) have been used to effect autonomic healing of various polymers.

[*] Dr. S. Chen, Prof. Dr. W. H. Binder
Institute of Chemistry, Chair of Macromolecular Chemistry
Faculty of Natural Sciences II
Martin-Luther-Universität Halle-Wittenberg
von Danckelmann-Platz 4, 06120 Halle (Saale) (Germany)
E-mail: wolfgang.binder@chemie.uni-halle.de
Dr. N. Mahmood, Prof. Dr. M. Beiner
Institute of Physics, Faculty of Natural Sciences II
Martin-Luther-Universität Halle-Wittenberg
Kurth-Mothes-Strasse 2, 06120 Halle (Saale) (Germany)
Prof. Dr. M. Beiner
Fraunhofer Institut für Werkstoffmechanik IWM
Walter-Hülse-Straße 1, 06120 Halle (Saale) (Germany)

[**] This research was supported by the Deutsche Forschungsgemeinschaft, DFG project BI 1337/7-1, the projects BI1337/8-1 and 1337/8-2 within the SPP 1568 ("Design and Generic Principles of Self-Healing Materials"), and the project A3 within the collaborative research center SFB TRR 102.

Supporting information for this article is available on the WWW under http://dx.doi.org/10.1002/anie.201504136.

However, the use of materials containing dynamic bonds implies poor shape persistence and a loss of mechanical performance since such materials often display gel-like properties. This disadvantage can be avoided by incorporating additional constraints or a "hard" phase that introduces shape persistence into the material.[6] Cluster formation,[3e,7] partial covalent crosslinking,[8] microphase separation,[9] or the introduction of nanocomposite principles[10] are possible strategies to generate self-healing materials that bear both multiple healing and shape-persistence properties. In particular, microphase separation has proven to be a viable strategy to generate stiffer materials that combine a hard phase with a higher glass-transition temperature (T_g) and a soft, low-T_g phase containing the supramolecular moiety that induces self-healing. Thus several research groups have studied the self-healing capabilities of microphase-separated polymers containing soft and hard domains by using computational models[11] or experimental approaches.[9,10,12]

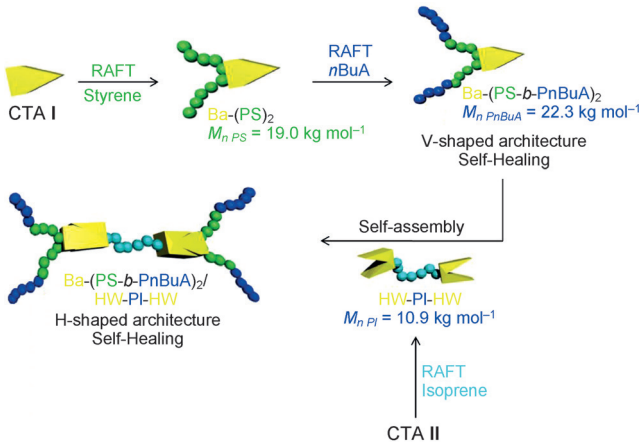

Figure 1. Strategy for preparing the V- and H-shaped supramolecular architectures by RAFT polymerization using CTA **I** and CTA **II**.

Herein we report the synthesis and properties of two novel self-healing materials generated from a V-shaped soft–hard–soft triblock copolymer functionalized with a barbiturate (Ba) unit in the center, and a subsequently generated H-shaped supramolecular architecture (Figure 1). The molecular design is based on thermoplastic elastomers (TPEs) with the difference that soft–hard–soft block copolymers are designed so that the supramolecular healing motif (Ba) is placed in the center of the hard middle block (V-shape, Ba(PS-*b*-P*n*BuA)$_2$). Although Ba is a significantly weaker

hydrogen-bonding motif than other supramolecular systems (such as 2-ureido-4-pyrimidinone (UPy)[12a]), we have obtained a material with good mechanical and excellent self-healing properties by the Ba-driven reversible formation of hydrogen-bonded associates. Furthermore, the precisely defined design and synthesis offers a suitable macromolecular building block to further construct the H-shaped supramolecular architecture by self-assembling with heterocomplementary HW-PI-HW. Our synthetic strategy towards soft–hard–soft triblock copolymer relies on a reversible addition fragmentation chain transfer (RAFT) process, where poly(*n*-butyl acrylate) (P*n*BuA) has been chosen as the soft block and polystyrene (PS) as the hard block, denoted as Ba-(PS-*b*-P*n*BuA)$_2$. Subsequent addition of another material property, achieved by blending with another soft polymer (HW-PI-HW), furnishes the corresponding H-shaped architecture. We subsequently investigated the rheological properties, the kinetics of hydrogen-bond formation, and the self-healing properties of both the V- and regular H-shaped supramolecular architectures (Figure 1).

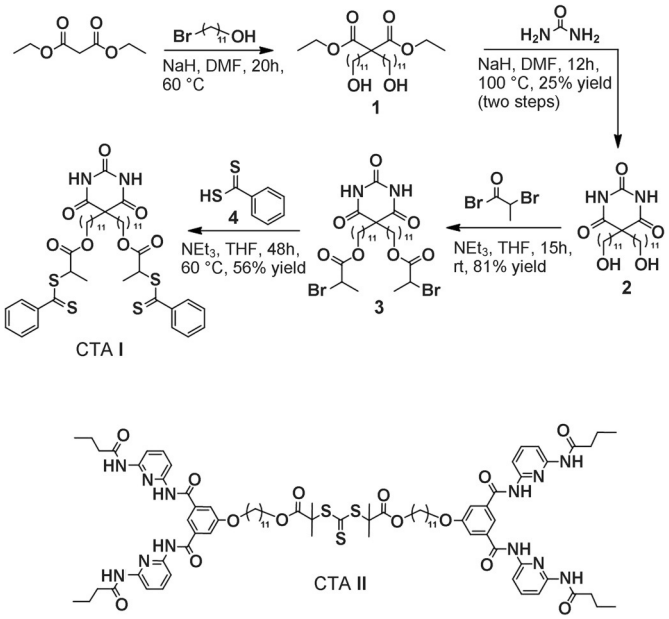

Scheme 1. Synthetic route for the preparation of the CTA **I** and structure of CTA **II**.

With the aim of developing the proposed self-healing materials based on dynamic supramolecular architectures, we initially designed the chain-transfer agent **I** (CTA **I**) functionalized with a Ba unit in the center and the α,ω-HW functionalized CTA **II**[13] (Figure 1). The synthesis of CTA **I** is realized as shown in Scheme 1, starting from the preparation of an undecanol disubstituted malonate **1**; subsequent reaction with urea generates compound **2** on a multigram scale (see Figure S1 in the Supporting Information), which is then converted into the dibromoester **3** (Figure S2), followed by bis-substitution with dithiobenzoic acid **4** to generate the expected CTA **I** (see Figures S3–S5 for ^{1}H, ^{13}C NMR, and ESI-TOF MS spectra).

Initially, the capability of Ba-functionalized CTA **I** to associate through hydrogen-bonding interactions with α,ω-HW-functionalized CTA **II** was examined by ^{1}H NMR analysis (Figure S6), and the association constant (K_{ass}) was subsequently determined by isothermal titration calorimetry (ITC) to be $5.13\times10^4\,\text{M}^{-1}$ in $CHCl_3$ at 30 °C (Figure S7).

After demonstrating the supramolecular association between CTA **I** and **II**, the capability of CTA **I** to efficiently mediate the solution polymerization of different monomers (styrene and *n*BuA) to afford the respective hydrogen-bonding polymers was investigated. The molar masses and the corresponding polydispersity (PDI) of all the obtained polymers are given in the Supporting Information (see Table S1 and Figure S8). Solution polymerizations of styrene mediated by CTA **I** show a controlled polymerization behavior. Kinetic studies highlight a linear relationship between $\ln(1/(1-x))$ versus time (Figure S8 A), thus indicating a steadily growth of telechelic polymers with monomer conversion (Figure S8 B), with PDI indices remaining below 1.28. The good correlation between the theoretical molecular weight and the experimental values obtained from NMR and SEC analysis (Table S1 and Figure S8 C) also confirms the controlled character of RAFT polymerization.

The hard polystyrene block (Ba-(PS)$_2$, $M_{n\,SEC}=19\,900\,\text{g mol}^{-1}$, PDI = 1.22) was employed as macroRAFT agent for the fabrication of the soft–hard–soft triblock copolymers, and was further chain-extended with *n*BuA to introduce the soft block. As expected, the macroRAFT agent Ba-(PS)$_2$ efficiently mediated the polymerization of *n*BuA, and showed linear first-order kinetics with progressive shifts of the SEC traces towards higher molecular weight and low PDI, thus confirming that the polymerization is living, together with the successful generation of the triblock copolymers Ba-(PS-*b*-P*n*BuA)$_2$ functionalized with Ba at the center (Figure S8 D, E and Table S1). The effective incorporation of the Ba moiety in the center of the hard middle chain was shown by MALDI-TOF MS (Figure S9) and ^{1}H NMR analysis, with the appearance of the barbiturate NH protons at 7.91 ppm (Figure S10 A). The capability of the resulting V-shaped macromolecules to self-assemble into H-shaped supramolecular architectures was subsequently evaluated by ^{1}H NMR spectroscopy and ITC (Figure S10–S12).

In accordance with previous considerations,[14] thermogravimetric analysis (TGA) measurements showed that all the generated polymeric materials are stable until around 315 °C (Figure S13), which indicates a useful thermal stability for technical applications. Since previous reports and our findings have shown that it is difficult to directly observe the microphase-separated morphology between PS and P*n*BuA blocks by transmission electron microscopy and small-angle X-ray scattering (Figure S14) because of the low electronic contrast,[15] differential scanning calorimetry (DSC) was employed as an indirect technique to investigate the microphase separation of both V- and H-shaped architectures. As seen in Figure 2 A, Ba-(PS-*b*-P*n*BuA)$_2$ shows two T_g values, thus indicating the phase separation in block copolymers: the T_g located at about 51.1 °C is ascribed to the PS phase,[16] while the T_g of the P*n*BuA phase is severely broadened in the region between about −50 and 0 °C, comparable to other PS-*b*-

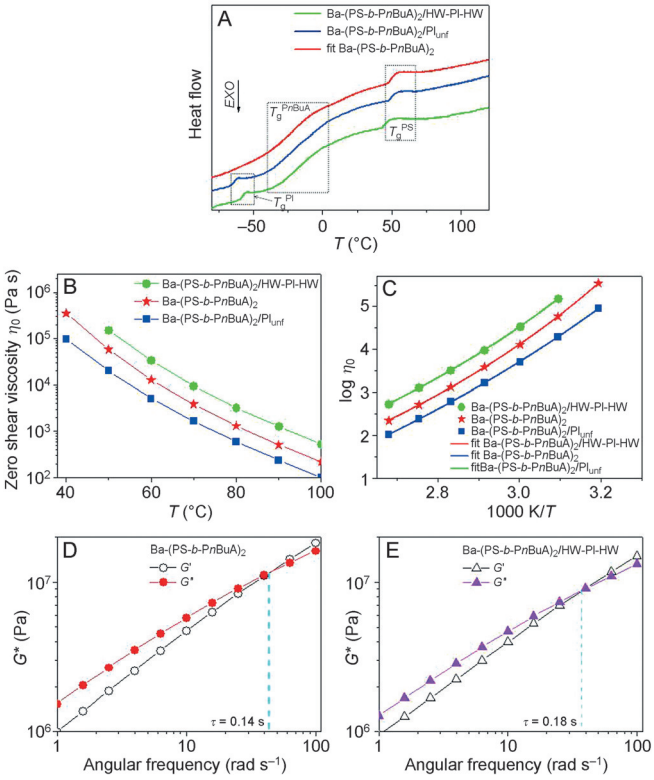

Figure 2. Characterization of the hydrogen-bonding polymers. A) Heat flow from DSC (2nd cycle). B) Zero shear viscosity (η_0) versus temperature. C) log η_0 versus 1000 K/T. D, E) Storage modulus (G') and loss modulus (G'') at 30 °C.

P*n*BuA-*b*-PS thermoplastic elastomers.[12a,15,17] In the case of a 2:1 blend (molar ratio) of Ba-(PS-*b*-P*n*BuA)$_2$ with unfunctionalized PI (PI$_{unf}$, $M_{n\,SEC} = 14\,100\ g\,mol^{-1}$, PDI = 1.12), in addition to the T_g of the PS and P*n*BuA phases, the emerging transition step at −63.6 °C corresponds to the PI phase. Replacing PI$_{unf}$ with hydrogen-bonding PI (HW-PI-HW) leads to shifts of the T_g values of the PS and PI phases to about 45.4 and −56.9 °C, respectively, thus indicating the successful formation of microphase segregated, self-assembled structures by hydrogen bonds between Ba-(PS-*b*-P*n*BuA)$_2$ and HW-PI-HW.

In order to achieve more insight into the relaxation dynamics of the individual components within the supramolecular materials,[18] frequency-dependent shear measurements at different temperatures (40–100 °C) were performed (Figure S15) on Ba-(PS-*b*-P*n*BuA)$_2$, the 2:1 blend of Ba-(PS-*b*-P*n*BuA)$_2$ with HW-PI-HW, or PI$_{unf}$ in the bulk state. From an extrapolation of these data to low frequencies, zero shear viscosities (η_0) could be determined in a broader temperature range (Figure 2B). As expected, the η_0 value decreases with increasing temperature and shows a non-Arrhenius-like temperature dependence in accordance with the Vogel–Fulcher–Tammann–Hesse equation[19] (VFTH; Table S2) for all samples (Figure 2C). The 2:1 blend of Ba-(PS-*b*-P*n*BuA)$_2$ with hydrogen-bonding PI (HW-PI-HW) displays higher η_0 values in comparison to both other samples, namely Ba-(PS-*b*-P*n*BuA)$_2$ and the 2:1 blend of Ba-(PS-*b*-P*n*BuA)$_2$ with PI$_{unf}$, in the entire temperature range where η_0 values are available, but with a quite similar temperature dependence (Figure 2B).

It is generally accepted that the lifetime of supramolecular bonds (τ), which is the characteristic average timescale for the reversible bonds to break and reform,[20] is correlated to the frequency (ω_i) where the storage modulus (G') and loss modulus (G'') curves intersect according to $\tau = 2\pi/\omega_i$.[21] The shear modulus as a function of frequency at 30 °C is shown in Figure 2D,E. An intercept point of $G'(\omega)$ and $G''(\omega)$ at ω_i could be observed for both Ba-(PS-*b*-P*n*BuA)$_2$ and the 2:1 blend of Ba-(PS-*b*-P*n*BuA)$_2$ with HW-PI-HW. The lifetime of the supramolecular bonds τ was calculated accordingly to be approximately 0.14 and 0.18 s for the corresponding samples, respectively (Figure 2D,E). As expected, this bond lifetime lies in the intermediate range (0.001–60 s) which is well situated in the known time range observed for supramolecular materials displaying responsiveness, adaptivity, and self-healing under certain conditions.[22]

In contrast to the neat HW-PI-HW sample, which could not be cast into free-standing films, both Ba-(PS-*b*-P*n*BuA)$_2$, and the 2:1 blend of Ba-(PS-*b*-P*n*BuA)$_2$ with HW-PI-HW are

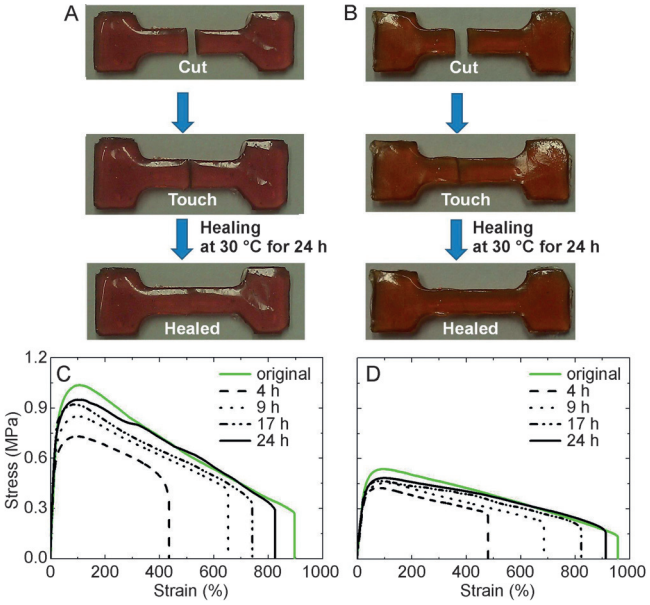

Figure 3. Self-healing tests for Ba-(PS-*b*-P*n*BuA)$_2$ (A, C), and Ba-(PS-*b*-P*n*BuA)$_2$/HW-PI-HW (2:1 blend; B, D).

capable of forming robust films. Thus the time-dependent self-healing tests are focused on Ba-(PS-*b*-P*n*BuA)$_2$, and the 2:1 blend of Ba-(PS-*b*-P*n*BuA)$_2$ with HW-PI-HW using stress–strain measurements (Figure 3).

Prior to evaluating the mechanical properties of healed samples, the original samples were first investigated in tensile tests. In general, Ba-(PS-*b*-P*n*BuA)$_2$ (Figure 3C, green curve), and 2:1 blend Ba-(PS-*b*-P*n*BuA)$_2$ with HW-PI-HW (Figure 3D, green curve) shows a low stress but high strain value at break. At the beginning of tensile tests, the stress increases and after about 100 % of the strain value, it decreases continuously until the break point, which is indicative of the stiff PS phase resisting the initial deforma-

Table 1: Physical properties of hydrogen-bonding polymers.

Sample	Young's modulus (MPa)	Original		After cutting and healing for 24 h		
		Breaking stress [MPa]	Breaking strain [%]	Breaking stress [MPa]	Breaking strain [%]	Breaking strain recovery [%]
Ba-(PS-*b*-P*n*BuA)$_2$	12.05 ± 0.23	0.27 ± 0.07	897 ± 32	0.29 ± 0.05	817 ± 27	91 ± 3
Ba-(PS-*b*-P*n*BuA)$_2$/HW-PI-HW	3.96 ± 0.05	0.13 ± 0.05	958 ± 43	0.16 ± 0.04	909 ± 30	95 ± 3

tion. Ba-(PS-*b*-P*n*BuA)$_2$ has a Young's modulus of approximately 12 MPa, however its blend with HW-PI-HW shows a significantly lower value (ca. 4 MPa; Table 1). The blend sample also deforms with even lower stress values. In both cases, the tensile stress after reaching the maximal tensile strength decreases with a constant slope, which is indicative of chain slippage after overcoming the rupture forces.

Time-dependent healing tests were subsequently performed by cutting dog-bone-shaped specimen in half, and later gently putting the resulting two pieces back in contact for around 1 min, and then leaving them for a given time at 30 °C. This temperature is significantly lower than the T_g of the PS block (Figure 3 A,B). Fast reconnection between the two pieces as well as a satisfactory recovery of mechanical stress was observed. As expected, increasing the healing time results in a better healing of the cut specimen in both cases (Figure 3 C,D). For example, after healing for 4 h, Ba-(PS-*b*-P*n*BuA)$_2$ reaches around 48 % of the original strain at break. In case of a 2:1 blend of Ba-(PS-*b*-P*n*BuA)$_2$ with HW-PI-HW, around 50 % of the original strain at break is achieved. Approximate values of 72–73 % and 82–86 %, respectively, are obtained after 9 and 17 h healing time for the corresponding samples. For even longer healing times (24 h), both samples show impressive healing capabilities, with optimal healing of up to about 95 % of the original strain at break values and stress values that approach those of the original state (Table 1), at least for large deformations (strains > 400 %). Most importantly, the two samples healed for 24 h show a mechanical performance comparable to that of the original uncut samples.

In conclusion, we present the rational design of two new self-healing materials based on thermoplastic supramolecular block copolymer architectures: V-shaped soft–hard–soft functionalized with Ba at the center, and H-shaped supramolecular block copolymers. In both compounds, the supramolecular moiety is placed in the center of the hard middle block copolymer, and both display dynamic and self-healing properties, with a nearly complete recovery of the initial mechanical performance within 24 h healing at 30 °C. The successful supramolecular blending strategy enables the generation of nearly any material composition, where the self-healing properties of the final material are maintained. We envision that this new concept toward the design of healable polymers using complex supramolecular architectures may open up new opportunities in the field of self-healing and tunable polymer materials, where precise molecular structures and architectures determine the final material properties.

Keywords: block copolymers · hydrogen bonds · RAFT polymerization · self-healing materials · supramolecular chemistry

How to cite: *Angew. Chem. Int. Ed.* **2015**, *54*, 10188–10192
Angew. Chem. **2015**, *127*, 10326–10330

[1] a) *Self-Healing Polymers. From Principles to Applications* (Ed.: W. H. Binder), Wiley-VCH, Weinheim, **2013**; b) W. H. Binder, B. Pulamagatta, M. Schunack, F. Herbst, in *Biomimetic Principles in Macromolecular Science* (Ed.: G. Swiegers), Wiley, Hoboken, **2012**, pp. 323–366; c) D. Döhler, P. Michael, S. Neumann, W. H. Binder, *Chem. Unserer Zeit* **2015**, *49*, DOI: 10.1002/ciuz.201500686.

[2] a) F. Herbst, D. Döhler, P. Michael, W. H. Binder, *Macromol. Rapid Commun.* **2013**, *34*, 203; b) W. Binder, R. Zirbs, *Supramolecular Polymers and Networks with Hydrogen Bonds in the Main- and Side-Chain* in *Hydrogen Bonded Polymers* (Ed.: W. H. Binder), *Vol. 207: Advanced Polymer Science*, Springer, Berlin, **2007**, pp. 1–78; c) W. H. Binder, S. Bernstorff, C. Kluger, L. Petraru, M. J. Kunz, *Adv. Mater.* **2005**, *17*, 2824–2828.

[3] a) P. Cordier, F. Tournilhac, C. Soulie-Ziakovic, L. Leibler, *Nature* **2008**, *451*, 977; b) F. Tournilhac, P. Cordier, D. Montarnal, C. Soulié-Ziakovic, L. Leibler, *Macromol. Symp.* **2010**, *291–292*, 84; c) D. Montarnal, F. Tournilhac, M. Hidalgo, J.-L. Couturier, L. Leibler, *J. Am. Chem. Soc.* **2009**, *131*, 7966; d) D. Montarnal, P. Cordier, C. Soulié-Ziakovic, F. Tournilhac, L. Leibler, *J. Polym. Sci. Part A* **2008**, *46*, 7925; e) F. Herbst, S. Seiffert, W. H. Binder, *Polym. Chem.* **2012**, *3*, 3084.

[4] a) M. V. Biyani, E. J. Foster, C. Weder, *ACS Macro Lett.* **2013**, *2*, 236; b) M. Burnworth, D. Knapton, S. Rowan, C. Weder, *J. Inorg. Organomet. Polym. Mater.* **2007**, *17*, 91; c) S. Bode, R. K. Bose, S. Matthes, M. Ehrhardt, A. Seifert, F. H. Schacher, R. M. Paulus, S. Stumpf, B. Sandmann, J. Vitz, A. Winter, S. Hoeppener, S. J. Garcia, S. Spange, S. van der Zwaag, M. D. Hager, U. S. Schubert, *Polym. Chem.* **2013**, *4*, 4966.

[5] a) Y. Amamoto, H. Otsuka, A. Takahara, K. Matyjaszewski, *Adv. Mater.* **2012**, *24*, 3975; b) Y. Amamoto, J. Kamada, H. Otsuka, A. Takahara, K. Matyjaszewski, *Angew. Chem. Int. Ed.* **2011**, *50*, 1660; *Angew. Chem.* **2011**, *123*, 1698; c) Y. Higaki, H. Otsuka, A. Takahara, *Macromolecules* **2004**, *37*, 1696.

[6] a) P. Michael, D. Döhler, W. H. Binder, *Polymer* **2015**, *69*, 215; b) D. Döhler, H. Peterlik, W. H. Binder, *Polymer* **2015**, *69*, 264.

[7] a) F. Herbst, K. Schröter, I. Gunkel, S. Gröger, T. Thurn-Albrecht, J. Balbach, W. H. Binder, *Macromolecules* **2010**, *43*, 10006; b) T. Yan, K. Schröter, F. Herbst, W. H. Binder, T. Thurn-Albrecht, *Macromolecules* **2014**, *47*, 2122.

[8] a) B. Ghosh, K. V. Chellappan, M. W. Urban, *J. Mater. Chem.* **2011**, *21*, 14473; b) J. Ling, M. Z. Rong, M. Q. Zhang, *Polymer* **2012**, *53*, 2691; c) J. Ling, M. Z. Rong, M. Q. Zhang, *J. Mater. Chem.* **2011**, *21*, 18373.

[9] Y. Chen, A. M. Kushner, G. A. Williams, Z. Guan, *Nat. Chem.* **2012**, *4*, 467.

[10] J. R. McKee, E. A. Appel, J. Seitsonen, E. Kontturi, O. A. Scherman, O. Ikkala, *Adv. Funct. Mater.* **2014**, *24*, 2706.
[11] a) B. V. S. Iyer, I. G. Salib, V. V. Yashin, T. Kowalewski, K. Matyjaszewski, A. C. Balazs, *Soft Matter* **2013**, *9*, 109; b) B. V. S. Iyer, V. V. Yashin, T. Kowalewski, K. Matyjaszewski, A. C. Balazs, *Polym. Chem.* **2013**, *4*, 4927; c) B. V. S. Iyer, V. V. Yashin, M. J. Hamer, T. Kowalewski, K. Matyjaszewski, A. C. Balazs, *Prog. Polym. Sci.* **2015**, *40*, 121.
[12] a) J. Hentschel, A. M. Kushner, J. Ziller, Z. Guan, *Angew. Chem. Int. Ed.* **2012**, *51*, 10561; *Angew. Chem.* **2012**, *124*, 10713; b) Y. Chen, Z. Guan, *Polym. Chem.* **2013**, *4*, 4885; c) S. Yu, R. Zhang, Q. Wu, T. Chen, P. Sun, *Adv. Mater.* **2013**, *25*, 4912; d) K. Xu, H. An, C. Lu, Y. Tan, P. Li, P. Wang, *Polymer* **2013**, *54*, 5665.
[13] S. Chen, Y. Deng, X. Chang, H. Barqawi, M. Schulz, W. H. Binder, *Polym. Chem.* **2014**, *5*, 2891.
[14] *Polymer Handbook*, 4th ed. (Eds.: E. H. Immergut, J. Brandrup, E. A. Grulke), Wiley, Hoboken, **2003**.
[15] S. Jiang, L. Zhang, T. Xie, Y. Lin, H. Zhang, Y. Xu, W. Weng, L. Dai, *ACS Macro Lett.* **2013**, *2*, 705.
[16] a) R. D. Spaans, M. Muhammad, M. C. Williams, *J. Polym. Sci. Part B* **1999**, *37*, 267; b) J. F. Masson, S. Bundalo-Perc, A. Delgado, *J. Polym. Sci. Part B* **2005**, *43*, 276.
[17] S. Robin, O. Guerret, J.-L. Couturier, R. Pirri, Y. Gnanou, *Macromolecules* **2002**, *35*, 3844.
[18] S. Chen, D. Ströhl, W. H. Binder, *ACS Macro Lett.* **2015**, *4*, 48.
[19] H. Vogel, *Phys. Z.* **1921**, *22*, 645.
[20] E. B. Stukalin, L.-H. Cai, N. A. Kumar, L. Leibler, M. Rubinstein, *Macromolecules* **2013**, *46*, 7525.
[21] a) R. K. Bose, N. Hohlbein, S. J. Garcia, A. M. Schmidt, S. van der Zwaag, *Phys. Chem. Chem. Phys.* **2015**, *17*, 1697; b) R. K. Bose, N. Hohlbein, S. J. Garcia, A. M. Schmidt, S. van der Zwaag, *Polymer* **2015**, *69*, 228.
[22] T. Aida, E. W. Meijer, S. I. Stupp, *Science* **2012**, *335*, 813.

Received: May 6, 2015
Revised: June 5, 2015
Published online: July 1, 2015

